

# Gamma-Ray Burst jet dynamics and their interaction with the progenitor star

BY DAVIDE LAZZATI, BRIAN J. MORSONY AND MITCHELL C. BEGELMAN

*JILA, University of Colorado, 440 UCB, Boulder, CO 80309-0440, USA*

The association of at least some long gamma-ray bursts with type Ic supernova explosions has been established beyond reasonable doubt. Theoretically, the challenge is to explain the presence of a light hyper-relativistic flow propagating through a massive stellar core without losing those properties. We discuss the role of the jet-star interaction in shaping the properties of the outflow emerging on the surface of the star. We show that the nature of the inner engine is hidden from the observer for most of the evolution, well beyond the time of the jet breakout on the stellar surface. The discussion is based on analytical considerations as well as high resolution numerical simulations. Finally, the observational consequences of the scenario are addressed in light of the present capabilities.

**Keywords:** gamma rays: bursts – hydrodynamics – shock waves – supernovae: general

## 1. Introduction

The detection of supernova signatures in the late afterglow of GRBs (Galama et al. 1998; Stanek et al. 2003; Hjorth et al. 2003) has established, beyond reasonable doubt, that at least a fraction of classical long duration GRBs are associated to the final evolutionary stages of massive stars. Such discovery has triggered speculation on the mechanisms that allow a relativistic jet to form, propagate in the core of a massive star, reach the surface of the star, and expand in space without being choked by baryon entrainment.

These questions have been addressed mainly numerically, with increasingly sophisticated codes and powerful computers. Pioneering work (MacFadyen & Woosley 1999) showed that a light jet can propagate unpolluted through a massive star core by pushing the cold dense stellar material aside. The head of the jet propagates sub-relativistically inside the star, allowing for the shocked material to flow in a cocoon that surrounds and hydrodynamically collimates the outflow. These results were subsequently confirmed by more refined special-relativistic computations (Aloy et al. 2000; Zhang et al. 2003). Recently, Lazzati & Begelman (2005) showed with an analytical model that the interaction between the jet and the star must create time evolution in the jet properties as it reach the stellar surface, even if the energy release at the core of the star is constant.

In this paper, we show the results of high resolution two-dimensional simulations, performed with the special relativistic Adaptive Mesh Refinement (AMR) code FLASH. Simulations were targeted to investigate the role of the jet-star interaction in shaping the structural and temporal properties of the jet outside the star surface. We show that the jet propagation takes place in four phases, three

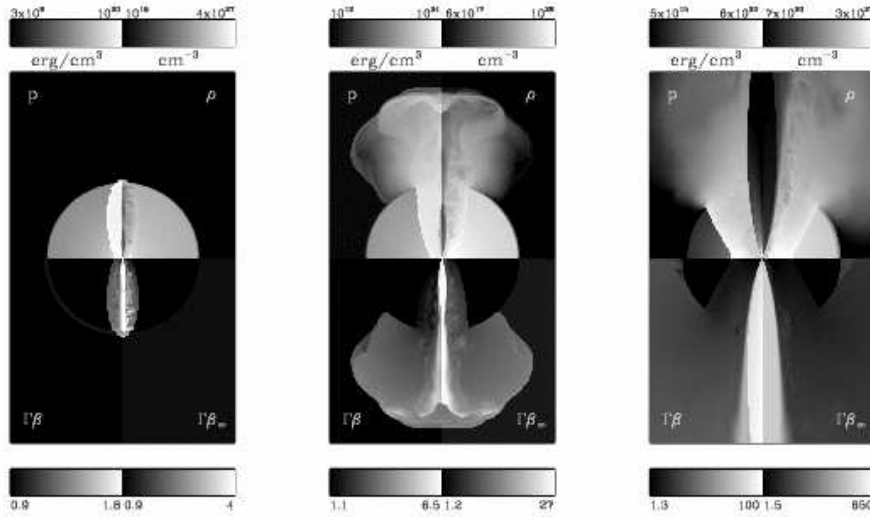


Figure 1. Stills from a simulation of a relativistic jet with  $\theta_0 = 10^\circ$ ,  $L = 1.33 \times 10^{51}$  erg s $^{-1}$ , and  $\Gamma_0 = 5$ . The jet propagates through a star with  $R = 10^{11}$  cm, a power-law density profile and a mass of  $M = 15M_\odot$ . Each of the three panels is divided into four sub-panels, each showing a different quantity. Starting from the upper right panel, in clockwise order, panels show the density, the Lorentz factor achievable at infinity, the actual Lorentz factor and the pressure. The gray-scale is always logarithmic. The first panel shows a still at 10.3 seconds after the moment at which the engine is turned on. The middle panel shows a still at 15 seconds, while the right panel shows a still at 40 seconds. The jet is in the shocked phase in the central panel and in the un-shocked phase in the right panel.

of which are radiative and can be observed in the GRB light curve. These phases can be separated by moments of quiescence, possibly explaining long dead-times observed between precursors and prompt emission in GRB light curves (Lazzati 2005). In contrast to previous lower resolution simulations, we find that the highly relativistic part of the jet can be well described with a sharp cutoff or with a top-hat toy model configuration. For more details about the code, the simulations, and some of the results reported here, see Morsony et al. (2006).

## 2. The simulations

With the aim of exploring the general properties of a confined light jet and of understanding the features introduced by a specific stellar progenitor we ran two different set of simulation. In one set, the star is described as a polytropic sphere with a power-law density profile  $\rho \propto r^{-2.5}$ . In a second set of simulations the stellar properties are taken from model 16TI of Woosley & Heger (2006), which is considered a possible GRB progenitor.

The jet injection is modeled as a boundary condition on the lower edge of the grid at  $10^9$  cm. The opening angle and Lorentz factor of the incoming jet are varied between simulations (we explore jets with injection opening angles between  $5^\circ$  and  $10^\circ$ ), but are constant at all times in each run. The terminal Lorentz factor, or Lorentz factor at infinity,  $\gamma_\infty$ , is defined as the Lorentz factor that the material would achieve if all its internal energy were converted to kinetic energy. It is cal-

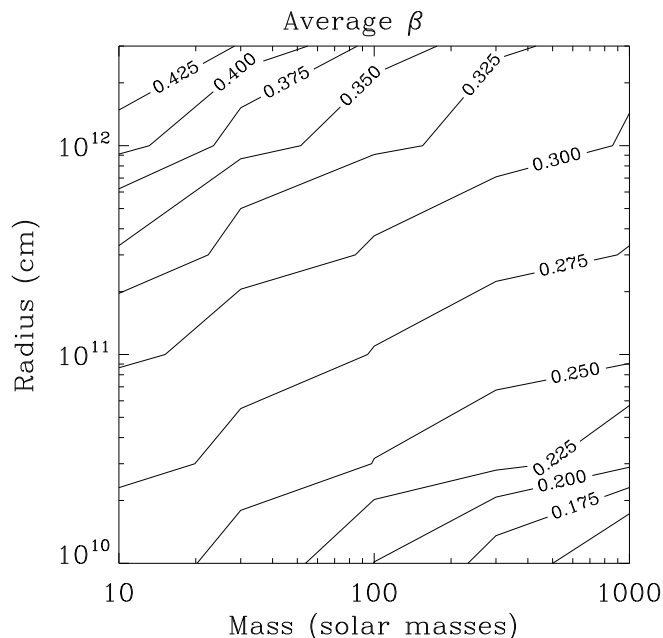


Figure 2. Average speed (in unit of the speed of light  $c$ ) of the propagation of the head of the jet through stars of different masses and radii. Computations are performed with the semi-analytic model developed by Morsony et al. (2006). Despite the large ranges in the stellar properties, the propagation speed is always close to  $0.3c$ . All jets have an initial opening angle of  $10^\circ$  and an injection Lorentz factor of 10.

culated as  $\gamma_\infty = (1 + 4p/\rho c^2)\gamma$ , where  $\gamma$  is the local bulk Lorentz factor.  $\gamma_\infty$  for the jet material is set to 400 for all simulations and the luminosity of the central engine is set to  $1.33 \times 10^{51} \text{ erg s}^{-1}$ . The injection Lorentz factor is either 2 or 5. Each simulation is run for 50 seconds, giving an energy input of  $6.65 \times 10^{52}$  ergs per jet, or a total energy of  $1.33 \times 10^{53}$  ergs assuming symmetric jets. These total energies are comparable to those assumed in previous works (see Zhang et al. 2003 for a discussion).

### 3. Results

A visual result of simulations are shown in Fig. 1. The figure shows stills of the simulation for a  $10^\circ$  jet propagating in a polytropic star with  $M = 15M_\odot$ . The figure (see also <http://rocinante.colorado.edu/~morsony/GRB/index.html> for animations) shows how the light relativistic jet propagates through the star and is affected by the propagation. The jet breaks on the stellar surface at approximately 10 seconds after the injection, releases a broad mildly relativistic component and eventually accelerate almost to its potential Lorentz factor of 400. We find that the jet propagation takes place in four phases, three of which are of great interest since are potentially radiative and can therefore be identified in the GRB light curve.

**The confined phase.** Initially the jet is confined inside the star. It immediately becomes supersonic and develops a shock structure at its head. The jet head

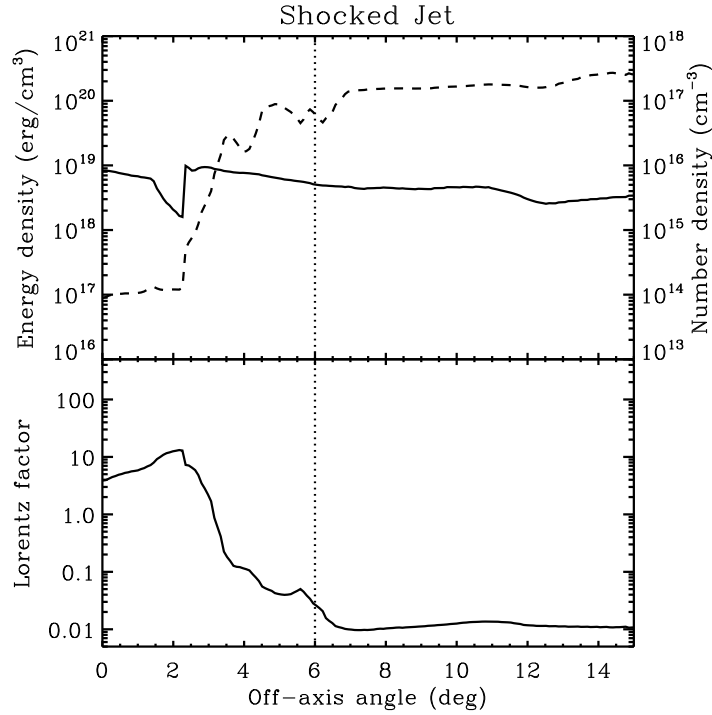


Figure 3. Cross section of the energy density and density (upper panel) and of the quantity  $\beta\Gamma$  of the shocked jet immediately outside the stellar surface. In the upper panel, the solid line and left y-axis show the energy density, while the dashed line and right y-axis show the density. The jet is characterized by variable properties and it is not easy to define a boundary between the jet and the outside.

propagates subrelativistically in the star, powered by the relativistic material behind that goes through the reverse shock. Since the head is sub-relativistic, and well in causal contact, the jet and stellar material do not accumulate but rather move backward to the sides of the jet, forming a high pressure cocoon. This cocoon pressure hydrodynamically collimates the jet (Begelman & Ciotti 1989). The jet propagation results therefore from the feedback between the head working surface, that increases the pressure of the cocoon, and the recollimation, that decreases the head surface and weakens the cocoon (Lazzati & Begelman 2005). Analytical considerations for a simple jet model (Morsony et al. 2006) suggest that the speed of the jet head is fairly independent on the stellar properties (see also Fig.2).

**The breakout.** As the head of the jet reaches the surface of the star, it opens a channel through which the hot material stored in the cocoon can escape. The cocoon material is dominated by the radiation energy and can in principle accelerate to relativistic speed. Its asymptotic Lorentz factor is, however, lower than that of the jet due to mixing with the stellar baryons. Unlike the jet material, the cocoon material is released through a nozzle on the surface of the star. As a consequence the cocoon material forms a quasi-spherical fireball. Taking advantage of the constancy

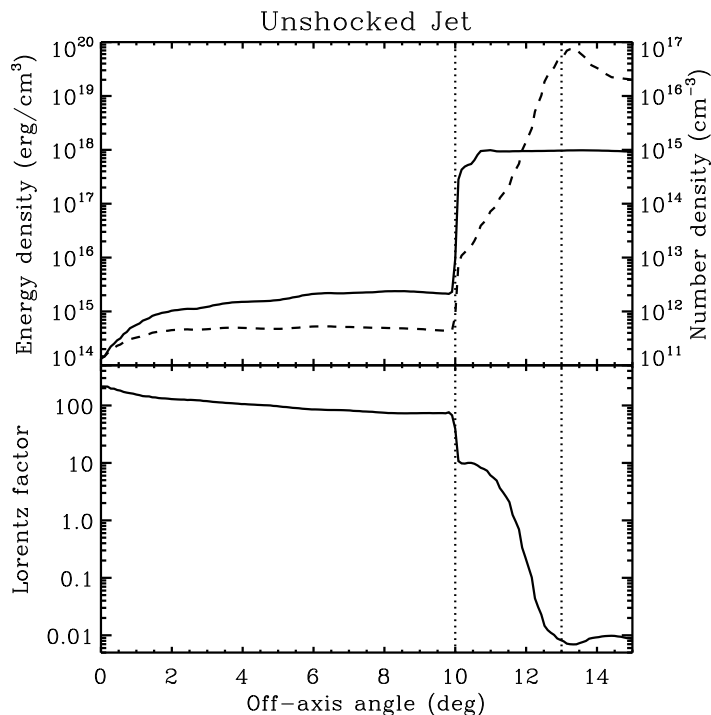


Figure 4. Same as Fig. 3 but for the un-shocked jet. In this case, a clear structure can be identified. The core of the jet is freely expanding with high Lorentz factor, and is separated from the outside by a boundary layer and a shock within which the density and speed of the material continuously approach the outside one.

of the propagation speed of the jet, we can evaluate the cocoon energy to be:

$$E_{\text{cocoon}} = L_j \left( t_{\text{br}} - \frac{R}{c} \right) \sim 2.3 L_j \frac{R}{c} \sim 10^{51} L_{j,50} R_{11} \quad (3.1)$$

The energy stored in the cocoon can give rise to a precursor (Ramirez-Ruiz et al. 2002ab). A measurement of the precursor energy can therefore give us valuable informations on the stellar dimension, assuming a radiative efficiency.

**The shocked jet.** As mentioned above, as the jet propagates in the confined phase, it is recollimated with tangential shocks. The first phase of jet propagation outside the star is therefore characterized by a jet whose structure is severely affected by the presence of multiple shocks. Figure 3 shows a cross section of the jet properties during the shocked phase. The cross section is taken just outside the stellar surface, and the star model is again the polytropic one. The jet in the figure is not clearly defined, and the vertical dashed line is somewhat arbitrary. There are shocks inside the jet boundary and the properties of the material are highly variable. The opening angle during this phase is somewhat constant, with small variations overlaid (see Morsony et al. 2006).

**The un-shocked jet.** The simulations show that several tens of seconds after the jet breaks out of the star surface, its configuration relaxes to a much more stable one. As can be seen in Fig. 4, the core of the jet is made by a free streaming outflow,

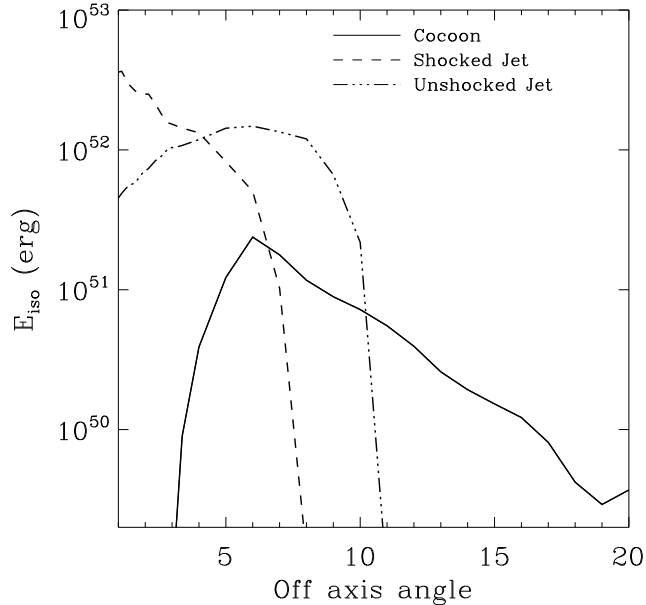


Figure 5. Energy distribution of the material ejected from the star in the three radiative phases. The y-axis shows the isotropic equivalent energy in ergs.

accelerating according to the adiabatic expansion  $\Gamma \propto r$ . It is unclear whether the feature in the very core of the jet is due to the dimensionality of the computations or is physics. This free streaming part of the jet is clearly bounded by a strong shock. The pressure of the material outside the shock is balanced by the jet ram pressure. The shocked area constitutes the boundary layer between the unperturbed core and the non-relativistic material outside. Inside the boundary layer, the density and Lorentz factor of the material join smoothly with the outside. The width of the layer is loosely associated to its highest Lorentz factor:  $\delta\theta \sim 3^\circ \sim 1/15$ . The inner free streaming part of the jet is very interesting since its propagation is unperturbed from the inner engine out to the radiative phase. As a consequence, it would be very interesting to isolate this component in observations and study its variability in order to gain information on the processes that take place at the very core of the star, where the jet is released and energized.

**The angular structure** The three phases of jet propagation outside the star are also characterized by a different angular structure, or energy distribution  $dE/d\Omega$ . During the prompt phase any given observer receives radiation produced only from the material moving along its line of sight. As a consequence, different observers will see different contribution from the three phases.

Figure 5 shows the energy distribution in the three phases as a function of the off-axis angle. Let us first consider an on-axis observer. He will see a very dim precursor, if any. This is due to the lack of energy emission in the isotropic precursor along the jet axis. It is not entirely clear whether this is an artifact of the 2D simulations or it is intimately linked to the process of vortex shedding that shapes the cocoon (Morsony et al. 2006). Immediately after the precursor, if any, the

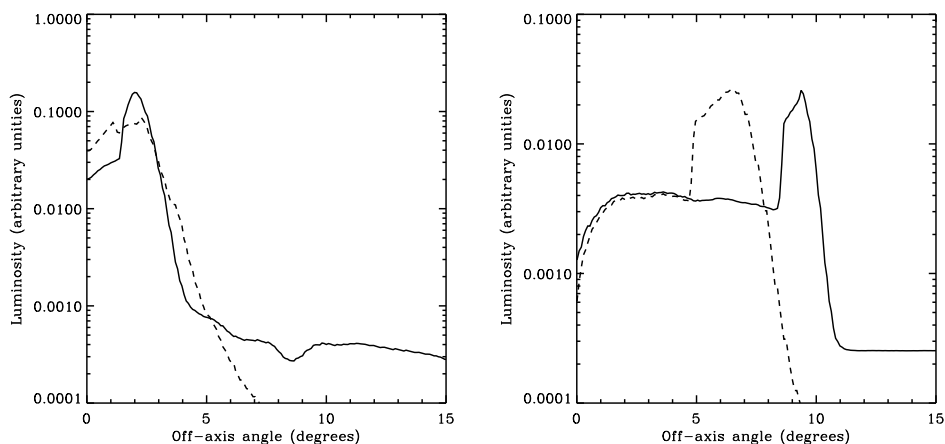


Figure 6. Evolution of the energy distribution over a factor of two in radius for the shocked jet (left panel) and un-shocked jet phases (right panel). Each panel shows with a solid line the energy distribution at the star surface ( $10^{11}$  cm) at time  $T$ . A dashed line shows instead the distribution of the same material at  $r = 2 \times 10^{11}$  cm at time  $T + 3.33$  s. The vertical axis is in arbitrary units. Data are from the polytropic star simulations.

on-axis observer will enter a very bright phase, during which the flow is dominated by the shocked jet. This is very well collimated material, concentrated at small angles. It is also characterized by strong variability (see Fig. 3) imprinted by the recollimation shocks. It should therefore be a favorable phase for the production of  $\gamma$ -rays through internal shocks and/or other dissipation mechanisms. Finally, the on-axis observer will see emission from the un-shocked jet. This emission is weak since most of the energy in the un-shocked phase is stored in the boundary layer. Even though the opening angle of the jet increases in time (Lazzati & Begelman 2005), the luminosity of the unshocked part of the jet is constant because the freely expanding material is not in causal contact with the jet boundary. During this phase no variability is imprinted in the flow by the interaction with the star. On the other hand, this is the phase in which the intrinsic variability of the inner engine, if any, is preserved.

Observers located at intermediate angles, with  $8^\circ < \theta < 11^\circ$  in Fig. 5, will experience a completely different emission pattern. They will see a relatively bright precursor, followed by a dark phase. During the shocked jet phase the jet is too collimated and no emission is observed at those angles. Eventually, as the jet enters the un-shocked phase, its opening angle spreads and the observer can see a bright GRB. The dead time will be in this case longer than any timescale associated with the jet or the central engine, and this effect could explain the early precursors observed with BATSE (Lazzati 2005) and Swift.

Finally, observers located outside the maximum opening angle of the jet (about  $11^\circ$  in the case of Fig. 5), will only see the precursor. Whether this weak emission could explain the observation of faint events like GRB 980425 and GRB 031203 is however a matter of open debate (e.g., Waxman, 2004)

There are two caveats to this discussion. First, the relative normalization of the curve in Fig. 5 can be changed significantly. Especially, the un-shocked jet phase can

last an arbitrarily long time, and therefore can dominate most of the emission. It is however unlikely that the inner engine will be fueled for much longer than several hundred seconds and therefore the figure should give a fairly correct representation of the energy budgets. Also, the normalization of the first two phases is somewhat related to the stellar radius and can therefore vary by approximately a factor 10.

More importantly, the energy distributions plotted in Fig. 5 are computed just outside the stellar radius, at several  $\times 10^{11}$  cm. The material has to travel out to the transparency radius, located at approximately  $10^{13}$  cm, before the GRB photons are produced. To what extent the energy distribution will be modified by the expansion over two orders of magnitude in distance is unclear. To estimate whether there will be sizable modifications we show in Fig. 6 the changes in the energy distribution over a factor 2 in radius. The left panel shows the case of the shocked jet, while the right panel shows the un-shocked jet. In both panels we select a thin shell in the outflow and we follow it through the expansion over a factor of two in radius, from  $10^{11}$  cm to  $2 \times 10^{11}$  cm. The shocked jet is only marginally modified during the expansion, the main effect being the filling of an energy minimum in the center. The un-shocked jet, instead, changes significantly. In particular, the strong shock that separates the freely expanding flow from the boundary layer moves inward (in angular coordinates), reducing the size of the freely flowing outflow. It seems unlikely that this shrinking can proceed to completely choke the free jet, but it is clear that energy distributions in the un-shocked jet phase should be taken with some caution.

#### 4. Summary

We presented high resolution numerical simulations of the hydrodynamic propagation of a light relativistic jet through a massive star, performed with the AMR code FLASH. We inject the jets as boundary conditions at the base of the grid and follow their propagation through the star, leaving the engine active for a timescale much longer than the time it takes the jet to break out on the stellar surface. We identify four phases of the jet propagation, three of which are radiative and can possibly contribute to the GRB light curve.

We describe the temporal and angular properties of the outflow in these three phases, showing how the outflow is initially very wide (the precursor phase, caused by the release of the cocoon on the stellar surface). Following this initial release, the jet emerges from the star hydrodynamically re-collimated by tangential shocks, producing a very bright highly collimated and variable jet. Eventually, as the stellar influence disappears with the cocoon release, the jet set into a stable condition whereby the core is freely expanding and is surrounded by a boundary layer that connects the highly relativistic core to the static dense stellar material. The jet opening angle grows steadily in this phase. Such a scenario allows us to explain the presence of long dead-time between the precursor emission and the subsequent main GRB discovered by Lazzati (2005) in approximately 20 per cent of bright BATSE light curves.

The software used in this work was in part developed by the DOE-supported ASC/Alliance Center for Astrophysical Thermonuclear Flashes at the University of Chicago. This work was supported by NSF grant AST-0307502, NASA Astrophysical Theory Grant NNG06GI06G, and Swift Guest Investigator Program NNX06AB69G. This work was partially supported



by the National Center for Supercomputing Applications under grant number AST050038 and utilized the NCSA Xeon cluster.

## References

- Aloy M. A., Müller E., Ibáñez J. M., Martí J. M., MacFadyen A., 2000, ApJ, 531, L119  
Begelman M. C., Cioffi D. F., 1989, ApJ, 345, L21  
Galama T. J., et al., 1998, Nature, 395, 670.  
Hjorth J., et al., 2003, Nature, 423, 847.  
Lazzati D., 2005, MNRAS, 357, 722  
Lazzati D., Begelman M. C., 2005, ApJ, 629, 903.  
MacFadyen A. I., Woosley S. E., 1999, ApJ, 524, 262.  
Morsony B. J., Lazzati D., Begelman M. C., 2005, ApJ submitted (astro-ph/0609254)  
Ramirez-Ruiz E., MacFadyen A. I., Lazzati D., 2002a, MNRAS, 331, 197  
Ramirez-Ruiz E., Celotti A., Rees M. J., 2002b, MNRAS, 337, 1349  
Stanek K. Z., et al., 2003, ApJ, 591, L17.  
Waxman E., 2004, ApJ, 602, 886  
Woosley, S. E. & Heger, A., 2006, ApJ, 637, 914  
Zhang W., Woosley S. E., MacFadyen A. I., 2003, ApJ, 586, 356.